The EMBO Journal Vol.18 No.17 pp.4633–4644, 1999

Impaired retinal function and vitamin A availability in mice lacking retinol-binding protein

Loredana Quadro[1,2], William S.Blaner[3], Daniel J.Salchow[4], Silke Vogel[3], Roseann Piantedosi[3], Peter Gouras[4], Sarah Freeman[4], Maria P.Cosma[2], Vittorio Colantuoni[2,5,6] and Max E.Gottesman[1,6]

[1]Institute of Cancer Research, [3]Department of Medicine and [4]Department of Ophthalmology, Columbia University, College of Physicians and Surgeons, New York, NY 10032, USA and [2]Department of Biochemistry and Medical Biotechnologies, University of Naples, Via Pansini 5, 80131 Naples, Italy

[5]Present address: Faculty of Biological Sciences, University of Sannio, 82100 Benevento, Italy

[6]Corresponding authors
e-mail: gottesma@cuccfa.columbia.edu or colantuoni@dbbm.unina.it

Retinol-binding protein (RBP) is the sole specific transport protein for retinol (vitamin A) in the circulation, and its single known function is to deliver retinol to tissues. Within tissues, retinol is activated to retinoic acid, which binds to nuclear receptors to regulate transcription of >300 diverse target genes. In the eye, retinol is also activated to 11-*cis*-retinal, the visual chromophore. We generated RBP knockout mice (RBP$^{-/-}$) by gene targeting. These mice have several phenotypes. Although viable and fertile, they have reduced blood retinol levels and markedly impaired retinal function during the first months of life. The impairment is not due to developmental retinal defect. Given a vitamin A-sufficient diet, the RBP$^{-/-}$ mice acquire normal vision by 5 months of age even though blood retinol levels remain low. Deprived of dietary vitamin A, vision remains abnormal and blood retinol declines to undetectable levels. Another striking phenotype of the mutant mice is their abnormal retinol metabolism. The RBP$^{-/-}$ mice can acquire hepatic retinol stores, but these cannot be mobilized. Thus, their vitamin A status is extremely tenuous and dependent on a regular vitamin A intake. Unlike wild-type mice, serum retinol levels in adult RBP$^{-/-}$ animals become undetectable after only a week on a vitamin A-deficient diet and their retinal function rapidly deteriorates. Thus RBP is needed for normal vision in young animals and for retinol mobilization in times of insufficient dietary intake, but is otherwise dispensable for the delivery of retinol to tissues.

Keywords: electroretinogram/high performance liquid chromatography/knockout mice/retinol-binding protein/vitamin A

Introduction

Retinoids (vitamin A and its analogs) are required for cellular proliferation, differentiation and apoptosis (Morris-Kay and Sokolova, 1996; Napoli, 1996). With the exception of vision, the all-*trans*- and 9-*cis*-isomers of retinoic acid are the active retinoid forms needed to support retinoid-dependent processes. Retinoic acid isomers regulate gene expression by binding to specific nuclear receptors, the retinoic acid receptors (RARs) and retinoid X receptors (RXRs), that function as ligand-dependent transcription factors (Chen and Evans, 1995; Kurokawa *et al*., 1995; Leblanc and Stunnenberg, 1995; Mangelsdorf *et al*., 1995; Pfahl and Chytil, 1996). Expression of >300 genes is influenced by retinoic acid availability (Gudas *et al*., 1994; Clagett-Dame and Plum, 1997). The retinoid used in the visual cycle is 11-*cis*-retinal (Wald, 1968), which forms a Schiff's base with opsin in photoreceptors to generate rhodopsin, the visual pigment. When excited by light, 11-*cis*-retinal isomerizes to all-*trans*-retinal. This light-catalyzed isomerization alters the conformation of opsin to expose G-protein-binding sites (Gregory-Evans and Bhattacharya, 1998), which induces a cascade of reactions resulting in a transmembrane hyperpolarization of the rods and/or cones (Baylor, 1996). This signal serves as the stimulus for second order neurons in the retina, which then transmit information to the next layer of neurons. Visual information is integrated in the central nervous system (Kelsey, 1997).

All retinoids present in the body originate from the diet (Blaner and Olson, 1994). Dietary retinoids are packaged by the intestine as retinyl ester, along with other dietary lipids, in chylomicrons. The majority of dietary retinoid is cleared by and stored within the liver (Vogel *et al*., 1999). To meet tissue retinoid needs, the liver secretes into the circulation retinol bound to a 21 kDa protein, retinol-binding protein (RBP). Crystallographic analysis of retinol–RBP from different species reveals a single retinol molecule buried within a highly conserved eight-stranded β-barrel structure (Soprano and Blaner, 1994; Newcomer, 1995). The retinol-binding site of RBP consists principally of amino acid residues coded by exons III, IV and V. The genomic organization of the RBP gene is also highly conserved across species (Soprano and Blaner, 1994).

Retinol-RBP is found in a 1:1 molar complex with a 55 kDa protein, transthyretin (TTR) (Monaco *et al*., 1995). This complex formation prevents retinol–RBP excretion by the kidney (Soprano and Blaner, 1994). The mechanism through which tissues acquire retinol from circulating retinol–RBP is subject to considerable debate. Membrane receptors for holo-RBP have been reported in the retinal pigment epithelium (RPE), in the placenta and in several other tissues and cells (Vogel *et al*., 1999). Such receptors could provide cells with a mechanism to regulate retinol uptake.

In the mouse embryo, RBP is synthesized as early as 7 days post-coitum (d.p.c.) by the visceral yolk sac,

consistent with a role for RBP in retinol delivery during embryogenesis (Johansson *et al*., 1997; Sapin *et al*., 1997). Developmental abnormalities were indeed induced in 7.5 d.p.c. embryos treated *in vitro* with antisense RBP mRNA (Bavik *et al*., 1996). RBP is also expressed in first trimester human placental membrane and in fetal liver (Marks *et al*., 1991).

Furthermore, except during severe vitamin A deficiency and in some disease states, retinol–RBP concentrations in the blood are maintained within narrow limits (Goodman, 1984; Helms *et al*., 1986; Matsuo *et al*., 1987; Holm *et al*., 1988; Winckler *et al*., 1989).

Based on these data, RBP is postulated to be essential for maintaining retinoid-dependent signaling pathways within the body.

To determine the role of RBP in retinoid physiology, we generated a mouse RBP knockout strain by targeted disruption of the genomic locus. The resulting RBP$^{-/-}$ mice are viable and fertile, but have reduced blood retinol levels, a marked but reversible impaired retinal function during the first months of life and impairment of retinol mobilization from hepatic stores.

Results

Targeted disruption of the RBP gene and generation of RBP$^{-/-}$ mice

A mouse RBP genomic fragment was used to construct a targeting vector. We replaced 591 bp of the RBP gene with a neomycin resistance cassette (*PMC1neo*), beginning 252 bp upstream of the TATA box and extending through exon I, intron I, exon II and 10 bp of intron II. The herpes thymidine kinase gene (*PMC1tk*) was inserted in the vector for counter-selection against non-homologous recombinants (Figure 1A). The targeting vector was linearized and electroporated into 129/Sv ES cells. After selection with G418 and gancyclovir, 570 resistant clones were isolated, expanded and screened by Southern blot. Genomic DNA was digested with *Bam*HI, *Hin*dIII and *Eco*RI and hybridized with four different probes: fragment A, encompassing exons III and IV; fragment B, containing exon V; the mouse RBP cDNA described below; and a 0.7 kb *Pst*I fragment of the *PMC1neo* cassette. Figure 1B shows a Southern blot with fragment A as probe indicating targeting of an RBP allele. This was confirmed by hybridizations with fragment B, the Neo probe and the mouse RBP cDNA (data not shown). The clone was injected into C57BL/6J blastocysts to generate male chimeras, scored by coat color. Chimeric mice were then bred with wild-type C57BL/6J females and germline transmission was confirmed by the agouti coat color of the offspring and by Southern blot analysis of their genomic DNA (Figure 1C). In a targeted 129/Sv allele, insertion of the *PMC1neo* cassette converts the wild-type 7 kb *Bam*HI fragment to a 7.5 kb fragment. In strain C57BL/6J, the wild-type allele yielded two bands of 3.6 and 3.4 kb, indicating the presence of a polymorphic *Bam*HI restriction site. This convenient polymorphism was used to follow the transmission of the wild-type C57BL/6J allele. Heterozygous mice yielded a 7.5 kb *Bam*HI fragment derived from the targeted allele and the two fragments derived from the C57BL/6J wild-type allele.

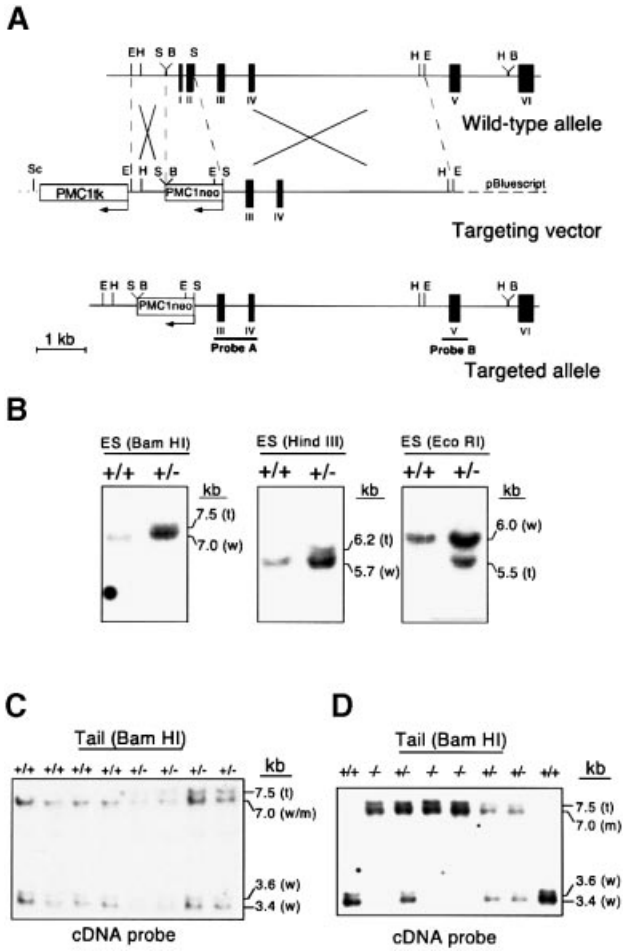

Fig. 1. RBP gene targeting. (**A**) Map of the RBP gene (top), gene targeting vector (middle) and RBP targeted allele (bottom). Exons are indicated by black boxes and Roman numerals. The *PMC1neo* and *PMC1tk* expressing cassettes, containing promoter and polyadenylation sequences, are indicated by white boxes. Arrows indicate the orientation of the transcription in the cassettes. The positions of relevant restriction sites for *Bam*HI (B), *Eco*RI (E), *Hin*dIII (H), *Sma*I (S) and *Sac*II (Sc) are indicated. The position of probe A (internal) and probe B (external) used to screen for homologous recombination events is indicated. (**B**) Southern blot of the ES cell positive clone (RBP$^{+/-}$). After *Bam*HI, *Hin*dIII or *Eco*RI digestion, probe A detects the wild-type (w) allele and the targeted (t) allele. (**C**) Southern blot of tail DNA from offspring of germline chimeras. After *Bam*HI digestion, the cDNA probe detects the C57BL/6J wild-type (w) allele (3.6 and 3.4 kb), the 129/Sv wild-type (w) allele (7 kb), the 129/Sv targeted (t) allele (7.5 kb) and the 129/Sv mutant (m) allele (7 kb). (**D**) Southern blot of tail DNA from offspring obtained from a cross of heterozygous mice. Genomic DNA was digested with *Bam*HI and hybridized with the cDNA probe. The C57BL/6J wild-type (w) allele (3.6 and 3.4 kb), the 129/Sv targeted (t) allele (7.5 kb) and the 129/Sv mutant (m) allele (7 kb) are indicated.

In addition, we detected a 7 kb *Bam*HI fragment that co-migrated with the wild-type 129/Sv allele. This fragment represents an RBP genomic rearrangement that occurred after exposure of the embryonic stem (ES) cells to the targeting vector (see below). Heterozygotes (RBP$^{+/-}$) were then mated to generate RBP knockout homozygotes (RBP$^{-/-}$) (Figure 1D). The RBP$^{-/-}$ mice were born at the expected Mendelian frequency, indicating that RBP is not essential for normal prenatal development. Furthermore, RBP$^{-/-}$ adults are viable and fertile.

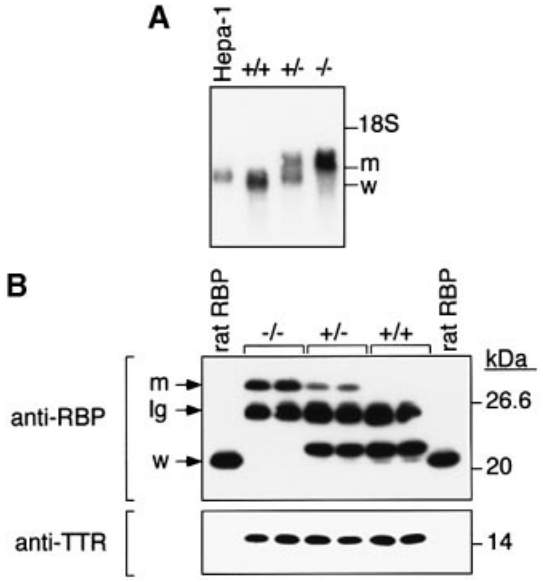

Fig. 2. Analysis of RBP mRNA and RBP protein in RBP$^{-/-}$ mice. (**A**) Northern blot analysis of total RNA (15 μg) extracted from mouse liver. As a positive control, 15 μg of total RNA from Hepa-1 cells (a mouse hepatoma cell line) was used. Wild-type (w) RBP mRNA, mutant (m) mRNA and the position of 18S rRNA are indicated. (**B**) Western blot analysis of protein from mouse plasma (5 μl of a 1:10 dilution of plasma). Rabbit polyclonal anti-rat serum RBP and rabbit polyclonal anti-rat serum TTR were used for immunodetection. A 100 ng aliquot of rat serum RBP purified to homogeneity was loaded as control. The position of protein markers is indicated. The wild-type 21 kDa RBP protein (w), the 28 kDa mutant protein (m), the cross-reacting light chain IgG (Ig) and the 14 kDa TTR monomer are also indicated.

Table I. Serum levels of RBP in RBP$^{+/+}$, RBP$^{+/-}$ and RBP$^{-/-}$ mice determined by RIA

Genotype	RBP (mg/dl)	*n*
RBP$^{+/+}$	3.5 ± 0.62	10
RBP$^{+/-}$	2.1 ± 0.60	10
RBP$^{-/-}$	ND	10

The values given represent mg of rat RBP equivalents and are means ± SD. ND = not detectable (<0.1 mg/dl). *n* = the number of male mice used.

Analysis of RBP RNA and protein in RBP$^{-/-}$ mice

Expression of the RBP gene was analyzed by Northern blot. Figure 2A shows RBP mRNA in total liver RNA from mice of all three genotypes. No wild-type RBP transcript was detected in RBP$^{-/-}$ mice. However, a transcript of ~1300 nucleotides (~400 nucleotides larger than RBP mRNA) was shown in RBP$^{+/-}$ and RBP$^{-/-}$ mice. Western blot analysis of blood samples from mice of all three genotypes, using a rabbit polyclonal anti-rat RBP antiserum, revealed no wild-type 21 kDa RBP protein in RBP$^{-/-}$ mice and showed a 28 kDa mutant protein in mice carrying the rearranged gene (Figure 2B). However, no immunoreactive protein was detected by radioimmunoassay (RIA) in the circulation of RBP$^{-/-}$ mice, using a sheep polyclonal anti-rat RBP antiserum (Table I). Western blot analysis also indicated that TTR levels were not affected by disruption of the RBP locus (Figure 2B).

Characterization of the function and structure of the 28 kDa protein

We reasoned that the 28 kDa mutant protein possessed little of the intact structure of RBP since the protein was not detected by an RIA carried out under non-denaturing conditions. Consequently, it was unlikely that the protein acted to transport retinol in RBP$^{-/-}$ mice. We confirmed this possibility through *in vivo* studies. We specifically asked whether the 28 kDa mutant protein functions to transport retinol in the RBP$^{-/-}$ mice. Since the small amounts of retinol present in the circulation of RBP$^{-/-}$ mice arise from recent dietary retinol intake (see below), six 3-month-old male RBP$^{+/+}$ and RBP$^{-/-}$ mice were each given by gavage a dose of [^{3}H]retinol in peanut oil. Ten hours after administration of this dose, a time when all chylomicron retinyl ester should be cleared from the circulation (Weng *et al*., 1999), the mice were sacrified and pools of RBP$^{+/+}$ and RBP$^{-/-}$ serum were obtained. Both serum pools (5310 ^{3}H c.p.m. in 0.5 ml of RBP$^{+/+}$ serum and 3520 ^{3}H c.p.m. in 0.5 ml of RBP$^{-/-}$ serum) were fractioned on the same Sephacryl S-200 gel filtration column. Fractions from the two column runs were taken for analyses of ^{3}H c.p.m. by scintillation counting, [^{3}H]retinol by HPLC and the presence of RBP or the 28 kDa mutant protein by Western blot analysis. As can be seen for RBP$^{-/-}$ serum (Figure 3), the concentration of the 28 kDa mutant protein was greatest in the two fractions (fractions 17 and 18) corresponding to the void volume of the column and progressively declined to an undetectable level by fraction 24. Immunoreactive 28 kDa protein could not be detected in any subsequent column fractions. Since tetrameric TTR would be expected to elute from this gel exclusion column with an elution volume corresponding to approximately those of fractions 30–35, the 28 kDa mutant protein cannot be bound to TTR in the circulation. ^{3}H c.p.m. first appeared in fractions 21 and 22 and reached a maximum level in fractions 25 and 26. This major peak of ^{3}H c.p.m. accounted for >90% of the ^{3}H c.p.m. applied to the column. A second minor peak of ^{3}H c.p.m. (<10% of the ^{3}H c.p.m. applied to the column) could be detected in column fractions 36–41. HPLC analysis of pooled fractions 21–29 indicated that the ^{3}H c.p.m. present in these fractions were present as [^{3}H]retinol. For wild-type serum (Figure 3C), the main peaks of ^{3}H c.p.m. and immunoreactive RBP co-eluted in fractions labeled M1 and M2 in Figure 3C, at an approximate volume at which the RBP–TTR complex would be expected to elute. A second minor peak of ^{3}H c.p.m. and immunoreactive RBP was also present in later fractions (Figure 3C, lane L) that eluted with the approximate volume expected for uncomplexed RBP. Neither ^{3}H c.p.m. nor immunoreactive RBP could be detected in fractions constituting the void volume (Figure 3C, lane V). Based on these data, we concluded that the 28 kDa protein must be present in the blood as part of a high molecular weight aggregate that does not function to transport retinol in the circulation. This conclusion was supported further by another *in vivo* binding experiment. Briefly, RBP$^{+/+}$ and RBP$^{-/-}$ mice were injected with [^{3}H]retinol, blood was taken and the percentage of circulating [^{3}H]retinol bound to RBP or to the 28 kDa mutant protein was determined. The results indicate that in the blood of RBP$^{+/+}$ mice, 10% of the total radioactivity was bound to RBP, whereas

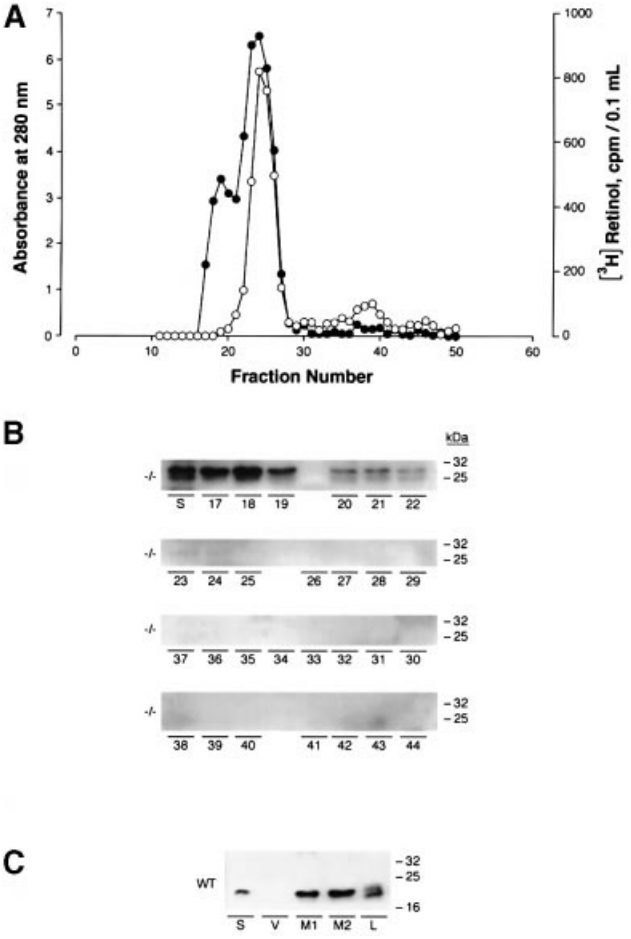

Fig. 3. Fractionation of serum from RBP$^{+/+}$ and RBP$^{-/-}$ mice by gel filtration chromatography. Serum (0.5 ml) was fractionated on a 1×50 cm column of Sephacryl S-200. The column was eluted with 10 mM sodium phosphate pH 7.2, containing 150 mM NaCl flowing at 4 ml/h. Each fraction contains 1.05 ml. Prior to the fractionation of the sera, the Sephacryl S-200 column had been calibrated with blue dextran, BSA and cytochrome *c*. For these chromatography conditions, the blue dextran first appeared in fraction 16; the BSA eluted at maximal concentration in fractions 24 and 25; and cytochrome *c* eluted at maximal concentration in fractions 40 and 41. (**A**) Elution profile for the fractionation of RBP$^{-/-}$ serum. The closed circles give absorbance at 280 nm and the open circles [^{3}H]retinol c.p.m. (**B**) Western immunoblot analysis of fractions 17–44 from (A) collected for fractionated RBP$^{-/-}$ mouse serum. The amount of protein loaded onto the SDS–polyacrylamide gel for each fraction (lane) was constant and consisted of ~1 μg protein. The lane designated 'S' is an aliquot of the serum pool collected from RBP$^{-/-}$ mice. The numbers under the other lanes correspond to the fraction numbers indicated in (A). The 32 and 25 kDa size markers for each SDS–polyacrylamide gel are given on the right. (**C**) Western immunoblot analysis for some fractions collected from the Sepharyl S-200 column following fractionation of a pool of RBP$^{+/+}$ mouse serum. The lane designated 'S' in (C) is an aliquot of the serum pool collected from RBP$^{+/+}$ mice. The lane marked 'V' corresponds to a pool of the void volume fractions 16 and 17; 'M1' to a pool of fractions 22–25; 'M2' to a pool of fractions 26–30; and 'L' to a pool of fractions 37–40. The mobilities of 32, 25 and 16 kDa size markers for this SDS–polyacrylamide gel are given on the right.

in the blood of RBP$^{-/-}$ mice the percentage of radioactivity associated with the 28 kDa mutant protein was at the experimental background level (1%; data not shown).

We also investigated the primary structure of the mutant 28 kDa protein following trypsin digestion and very sensitive matrix-assisted laser desorption/ionization-mass spectroscopic (MALDI-MS) analysis (Henzel *et al*., 1993). For this purpose, an immunoprecipitate of the 28 kDa protein was made employing the same rabbit anti-rat RBP antiserum used to detect the 28 kDa protein by immunoblot analysis. This immunoprecipitate was subjected to SDS–PAGE. Following staining of a lane of this polyacrylamide gel for protein with Coomassie Blue, the major protein band present on the gel, corresponding to the 28 kDa protein, was excised from the gel. The excised protein band was then subjected to proteolytic digestion with trypsin. The peptide fragments generated upon proteolysis subsequently were fractionated by MALDI-MS. Figure 4 provides the profile obtained from the mass spectrometer for these peptides and Table II provides a listing of the masses (m/z) that would be expected for peptides generated following complete and partial digestion of mature serum RBP (the arrows in Figure 4 provide the positions where these RBP fragments would be expected to be located upon mass spectroscopy). As can be seen from inspection of Figure 4 and Table II, none of the peptides detected upon MALDI-MS analysis showed masses (m/z) that would be expected for peptides generated from complete or partial digestion of native RBP. Considering that MALDI-MS has a low limit of detection of $<$500 fmol per peptide fragment, we conclude from this primary analysis that the mutant protein does not share extensive stretches of identity with RBP. To investigate further the primary sequence of the 28 kDa protein, we also carried out an analysis of the N-terminal sequence of the 28 kDa mutant protein (Ferrara *et al*., 1993). This analysis revealed, for the first 15 N-terminal amino acids of the 28 kDa protein, no similarity in the primary sequences for mouse RBP and the 28 kDa protein. No other similarities were detected for the 28 kDa protein and any other known sequences in the Swiss Protein Database (data not shown). Based on this sequence information for the 28 kDa protein, we hypothesize that it probably represents a frameshift fusing a small portion of RBP to an unknown open reading frame. The resulting polypeptide contains only a small stretch of the original RBP sequence. Accordingly, although the mutant DNA and mRNA were detected by Southern and Northern blot analysis, the mutant protein was recognized by the rabbit but not by the sheep anti-RBP antiserum.

Serum and tissue levels of retinol and retinyl esters in RBP$^{-/-}$ mice

Serum and tissue retinol and retinyl ester levels were measured by reverse phase HPLC for 13-week-old male and female animals. Serum retinol levels in RBP$^{+/-}$ mice were 50% those of RBP$^{+/+}$ mice, whereas the levels in RBP$^{-/-}$ mice were 12.5% of wild-type (Table III). No statistically significant differences in hepatic total retinol levels between RBP$^{-/-}$ and RBP$^{+/+}$ mice were observed (data not shown). Thus, at this age, the absence of RBP dramatically reduces serum retinol levels, but does not impair accumulation of hepatic retinol stores. No statistically significant differences in total retinol concentrations were observed in kidney, spleen, testis and ovary in 13-week-old RBP$^{+/+}$ and RBP$^{-/-}$ mice (data not shown). Serum and hepatic total retinol concentrations were also measured in 3-week- and 5-month-old RBP$^{+/+}$ and RBP$^{-/-}$ mice. Serum levels of retinol were consistently low

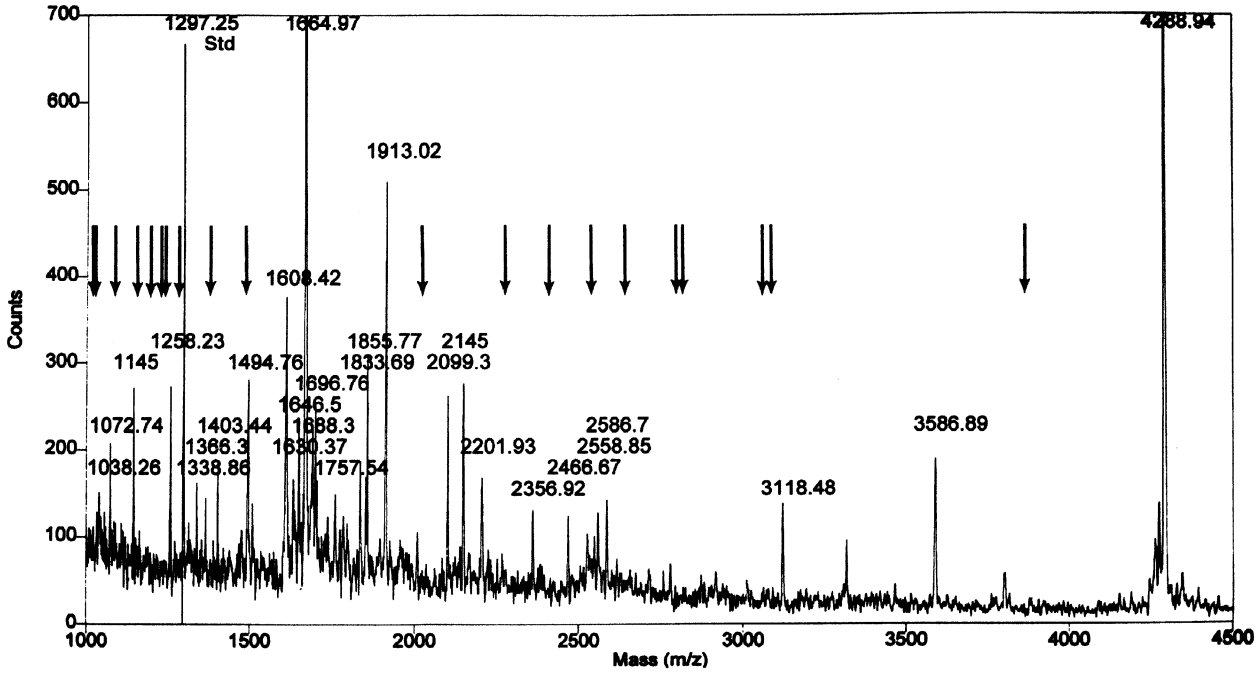

Fig. 4. MALDI-MS analysis of a trypsin digest of the 28 kDa mutant protein. The numbers on the figure represent the masses (m/z) for each of the tryptic fragments obtained after digestion of the 28 kDa protein and separation by mass spectroscopy. Only tryptic fragments with a mass (m/z) of >1000 are given in the figure. The arrows indicate the position where peptides generated upon complete or partial tryptic digestion of native mouse RBP would be expected to be found. A listing of the masses of RBP tryptic fragments generated upon complete or partial digestion of mouse RBP is provided in Table II. This mass spectroscopic analysis is able to detect peptides with a low limit of detection of <500 pmol. Thus, for peptides with masses (m/z) ranging between 1000 and 5000, as shown in this figure, we would expect to be able to detect peptides if they were present at a level as low 0.5–2.5 ng.

Table II. MALDI-MS analysis

Position	Predicted mass	Experimental mass
118–157	4654.996	4288.94
108–139	3858.192	3586.89
140–167	3091.335	3118.48
49–76	3064.393	2586.70
81–105	2819.173	2466.67
79–103	2799.142	2356.92
118–139	2649.807	2201.93
81–103	2543.822	2145.00
48–68	2408.667	2099.30
49–68	2280.493	1913.02
140–157	2024.212	1855.77
106–117	1486.774	1696.76
36–47	1383.635	1664.97
38–48	1284.543	1608.42
158–168	1242.334	1494.76
108–117	1227.408	1403.44
19–28	1196.323	1258.23
38–47	1156.369	1145.00
158–167	1086.146	1072.74
172–179	1019.160	–
69–78	1016.163	–

Comparison between the masses of the peptides obtained after tryptic digestion of the RBP protein (predicted mass) and those of the peptides obtained after tryptic digestion of the 28 kDa protein (experimental mass). The mass value (m/z) is expressed in Da. The first column indicates the position of the cleavage sites in the RBP protein.

(12.5%) in both age groups of $RBP^{-/-}$ mice (data not shown). Three-week-old $RBP^{-/-}$ and $RBP^{+/+}$ mice had equivalent liver total retinol concentrations (data not shown). However, 5-month-old $RBP^{-/-}$ mice had significantly higher hepatic retinol and retinyl ester levels than age- and sex-matched $RBP^{+/+}$ animals (Table IV). Thus, although serum retinol levels remain low with increasing age, $RBP^{-/-}$ mice accumulate more hepatic total retinol than wild-type controls. These observations suggest that retinol mobilization from hepatic stores may be compromised in $RBP^{-/-}$ mice.

Table III. Serum retinol levels in $RBP^{+/+}$, $RBP^{+/-}$ and $RBP^{-/-}$ mice

Genotype	Retinol[a] (μg/dl)	*n*
$RBP^{+/+}$		
M	25.6	2
F	16.5 ± 3.8	4
$RBP^{+/-}$		
M	15.6	2
F	9.5 ± 2.9	4
$RBP^{-/-}$		
M	2.7 ± 0.4	3
F	3.1 ± 1.1	4

[a]Retinol levels are determined by reverse phase HPLC and are expressed as μg/dl of serum ± SD (when >2 mice were analyzed). *n* = numbers of 13-week-old male (M) or female (F) mice analyzed.

$RBP^{-/-}$ mice have impaired retinal function

Because of the unique role of retinol in vision, we measured retinol levels in the eye cups of $RBP^{+/+}$ and $RBP^{-/-}$ mice at different ages by reverse phase HPLC. At 3 weeks, eye cup retinol content in $RBP^{-/-}$ mice was only 25% of wild-type. The eye cup retinol content of $RBP^{-/-}$ mice increased with age at the same rate as controls, but remained significantly lower for as long as 13 weeks

Table IV. Hepatic levels of retinol and retinyl esters in 5-month-old $RBP^{+/+}$ and $RBP^{-/-}$ mice

Genotype	Retinol[a] (μg/g)	Retinyl esters[b] (μg/g)	*n*
$RBP^{+/+}$	19.8 ± 6.5	700 ± 309	5
$RBP^{-/-}$	27.7 ± 19.6	1798 ± 1278	5

[a]Retinol levels are determined by reverse phase HPLC and are expressed as μg/g of tissue.
[b]Retinyl esters are determined by reverse phase HPLC and are expressed as retinol equivalents/g of tissue. The levels of each individual retinyl ester (retinyl palmitate, retinyl oleate, retinyl stearate and retinyl linoleate) were summed to provide the total retinyl ester levels. Values are given as means ± SD.
n = numbers of age- and sex-matched mice analyzed.

post-partum (Figure 5A). To determine whether $RBP^{-/-}$ mice had impaired visual function, we performed dark-adapted electroretinograms (ERGs). As shown in Figure 5B, 4-week-old $RBP^{-/-}$ mice displayed an abnormal ERG response. The threshold was elevated, i.e. more light was needed to elicit a threshold b-wave. Comparison of the b-wave amplitude of $RBP^{-/-}$, $RBP^{+/-}$ and wild-type mice (Figure 5C) reveals a 100-fold decreased (2 log units) sensitivity of the RBP knockout mice to light. The response to a maximal stimulus was about half of normal.

The retinal impairment of $RBP^{-/-}$ mice reverses with time

Dark-adapted ERG analysis of mice of different ages showed that the vision of $RBP^{-/-}$ animals progressively improved and approached that of wild-type animals. Figure 5D illustrates representative ERG responses of a $RBP^{-/-}$ mouse at different ages. Whereas the response at 4 weeks of age showed the typical abnormalities observed in young $RBP^{-/-}$ mice, ERG profiles from the same mouse at 24 weeks of age had a normal appearance, with a deep a-wave, a high b-wave and a rapid falling phase.

Analysis of retinol-derived metabolites in the eye cups of $RBP^{-/-}$ mice

Homogenates prepared from eye cups of 3-week-old $RBP^{-/-}$ and wild-type animals were assayed by normal phase HPLC for 11-*cis*-retinal, the retinol-derived metabolite required in the visual cycle, and retinyl ester. The level of 11-*cis*-retinal in age- and sex-matched $RBP^{+/+}$ mice averaged 57.3 ± 9.9 ng/pair of eye cups ($n = 5$), whereas the level in age- and sex-matched $RBP^{-/-}$ animals was only 10.7 ± 6.4 ng/pair of eye cups ($n = 5$). The low concentration of 11-*cis*-retinal is entirely consistent with the abnormal visual phenotype. This difference was still observed in 8-month-old $RBP^{-/-}$ animals compared with age- and sex-matched wild-type mice (87 ± 16 ng/pair of eye cups in $RBP^{+/+}$ mice and 49 ± 19 ng/pair of eye cups in $RBP^{-/-}$ animals; $n = 4$). Furthermore, retinyl ester levels were extremely low in 8-month-old $RBP^{-/-}$ animals, averaging 13 ± 5 ng/pair of eye cups, compared with 168 ± 32 ng/pair of eye cups in $RBP^{+/+}$ mice ($n = 4$). In contrast, eye cup retinol levels were identical in adult animals (53 ± 7 ng/pair eye cups in $RBP^{+/+}$ mice; 56 ± 13 ng/pair eye cups in $RBP^{-/-}$ mice).

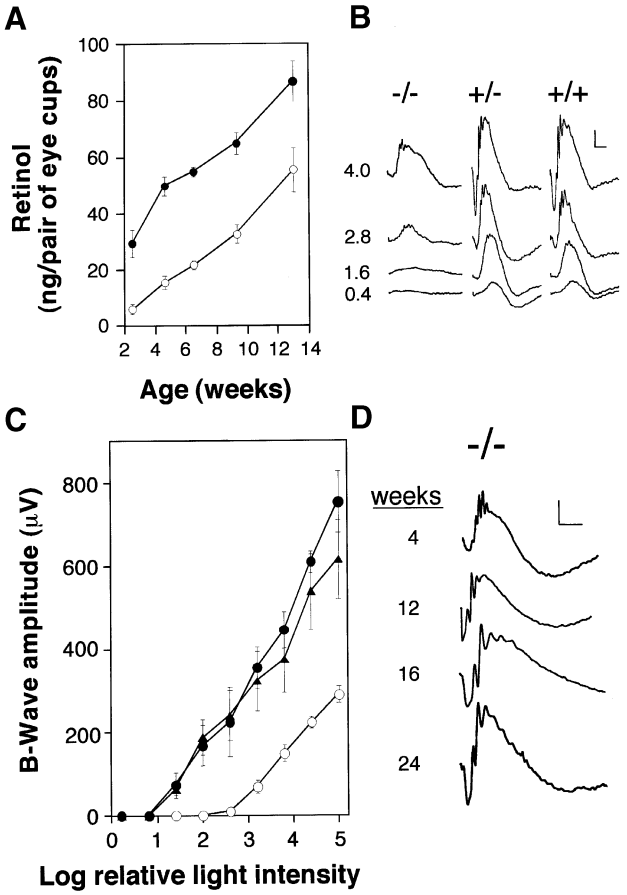

Fig. 5. Eye cup levels of retinol and analysis of retinal function for $RBP^{-/-}$ and $RBP^{+/+}$ mice. (**A**) Whole eye homogenates were analyzed by reverse phase HPLC to determine the levels of retinol in eye cups from $RBP^{-/-}$ (○) and $RBP^{+/+}$ (●) animals at different ages. The values are indicated as means ± SD for 3–5 mice. Error bars indicate the standard deviation. (**B**) Corneal ERG responses to stimuli of white light obtained from 3-week-old $RBP^{+/+}$, $RBP^{+/-}$ and $RBP^{-/-}$ mice that had been dark-adapted overnight. The scale indicates 150 μV vertically and 50 ms horizontally. The relative logarithmic light intensity of each flash is indicated on the left. (**C**) Relationship between the amplitude of the b-wave of the ERG in μV and the relative light intensity of the stimulus on a logarithmic scale. Values are given as the mean ± SE for six $RBP^{-/-}$ (○), four $RBP^{+/-}$ (▲) and three $RBP^{+/+}$ (●) mice at 3 weeks of age. Error bars indicate the standard error. (**D**) Representative corneal ERGs in response to white light stimuli at the maximal intensity for one $RBP^{-/-}$ mouse taken at different ages. The calibration bar indicates 150 μV vertically and 50 ms horizontally.

Origin of the residual serum retinol in $RBP^{-/-}$ mice

To ask whether the retinol in the circulation of $RBP^{-/-}$ mice arose from recent dietary intake, we placed these and control animals on a vitamin A-deficient diet. After 1 week, plasma retinol in $RBP^{-/-}$ mice fell from 12.5% of wild-type to undetectable levels (Figure 6C), whereas wild-type animals on the same diet maintained constant plasma retinol concentrations (data not shown). This indicates that the residual serum retinol in the knockout mice derives from recent dietary intake. Note that $RBP^{-/-}$ mice fed the vitamin A-sufficient diet showed a low peak of serum retinyl palmitate on HPLC analysis (Figure 6B). A similar peak, which derives from chylomicron-bound dietary retinyl ester, was observed for $RBP^{+/+}$ mice fed a control diet but not for $RBP^{-/-}$ mice maintained on a vitamin A-deficient diet (data not shown). The $RBP^{-/-}$

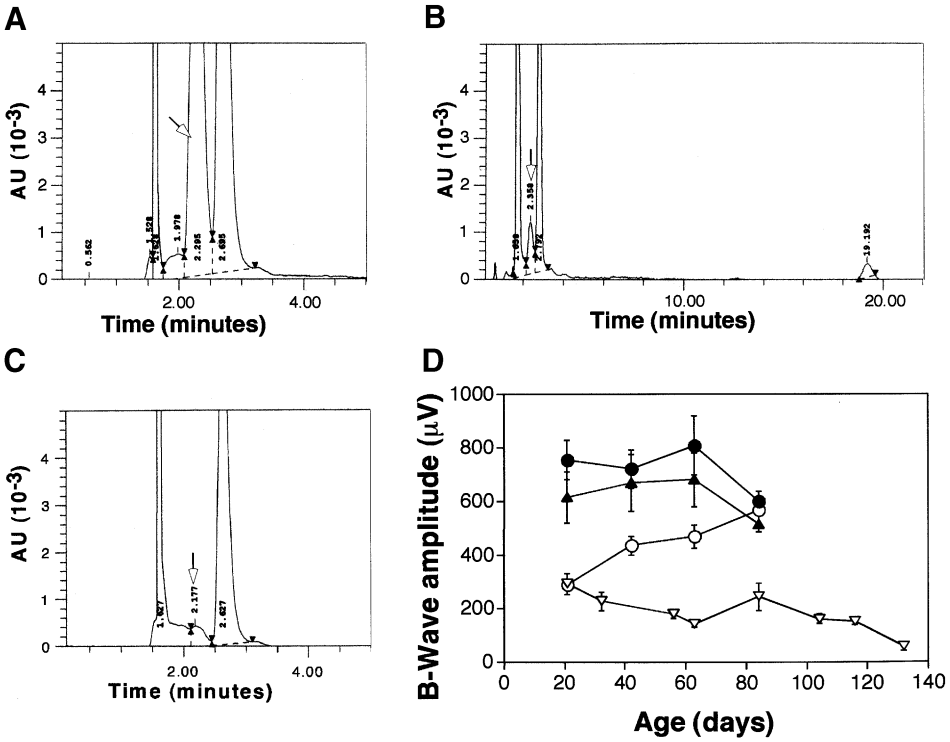

Fig. 6. Effects of vitamin A-deficient diet on plasma retinol levels and on retinal function. Representative reverse phase HPLC profiles for plasma retinol from $RBP^{+/+}$ (**A**) and $RBP^{-/-}$ (**B**) mice consuming a control vitamin A-sufficient diet and from a $RBP^{-/-}$ mouse (**C**) consuming a vitamin A-deficient diet for 1 week after maintenance throughout life on a vitamin A-sufficient diet. These age-matched mice were not fasted prior to sacrifice. For each of the HPLC profiles, the white arrow indicates the expected position of retinol, which elutes with a retention time of ~2.2 min. The peak eluting with a retention time of ~1.65 min corresponds to the solvent benzene and the peak eluting at 2.6–2.7 min corresponds to the internal standard retinyl acetate. In (B), the peak eluted with a retention time of ~19.2 min corresponds to retinyl palmitate. The scale of the vertical axis for each panel (A, B and C) is identical (absorbency units at 325 nm). The horizontal axis for the profile from $RBP^{-/-}$ mice consuming the control diet (C) is scaled differently to demonstrate the retinyl palmitate peak. (**D**) Relationship between the amplitude of the b-wave of the ERG in μV, in response to white light stimuli at the maximal intensity, as a function of the age of the mice. Analysis of $RBP^{+/+}$ (●), $RBP^{+/-}$ (▲) and $RBP^{-/-}$ (○) mice fed a vitamin A-sufficient diet and $RBP^{-/-}$ (△) mice fed a vitamin A-deficient diet. Values are given as the mean ± SE for three to five animals each per group. Error bars indicate the standard error.

Table V. Hepatic levels of total retinol in $RBP^{+/+}$ and $RBP^{-/-}$ mice after 7 days on a vitamin A-deficient diet

Genotype	Diet	Retinol[a] (μg/g)	*n*
$RBP^{+/+}$	control	281 ± 69	5
$RBP^{+/+}$	deficient	50 ± 22	5
$RBP^{-/-}$	control	177 ± 75	5
$RBP^{-/-}$	deficient	241 ± 63	5

[a]Retinol is determined as total retinol pool (retinol + retinyl esters) by reverse phase HPLC and is expressed as μg/g of tissue (retinyl ester concentration is determined as retinol equivalents/g of tissue). Values are given as means ± SD.
n = numbers of age- and sex-matched mice analyzed.

animals maintained for 7 days on the deficient diet and sex- and age-matched $RBP^{-/-}$ mice maintained for the same period on the control diet had equivalent hepatic total retinol levels (Table V). In contrast, hepatic total retinol concentrations fell significantly in $RBP^{+/+}$ mice maintained for 7 days on the vitamin A-deficient diet compared with sex- and age-matched $RBP^{+/+}$ mice maintained on the control diet (Table V). That the vitamin A-deficient diet induces a decline in serum retinol in $RBP^{-/-}$ mice without a compensating decrease in hepatic total retinol levels indicates that RBP is required to mobilize retinol from hepatic retinoid stores.

Effect of the daily dietary intake on the visual phenotype

To test the influence of dietary vitamin A intake on the visual phenotype, we monitored retinal function in $RBP^{-/-}$ and $RBP^{+/+}$ mice maintained on vitamin A-deficient or vitamin A-sufficient diets, starting at the time of the weaning (Figure 6D). At weaning (21 days of age), $RBP^{-/-}$ mice had a significantly lower b-wave than either wild-type or heterozygous mice. After 63 days on the control diet, the dark-adapted ERG response of $RBP^{-/-}$ mice was normal. In contrast, the b-wave amplitude of $RBP^{-/-}$ mice kept on a vitamin A-deficient diet progressively decreased (Figure 6D), their ERG threshold rose, the amplitude of the a-wave decreased and the falling phase was more prolonged. The ERG response of $RBP^{+/+}$ mice kept on a vitamin A-deficient diet remained unchanged throughout the experiment (data not shown). After 130 days on a vitamin A-deficient diet, in $RBP^{-/-}$ mice the b-wave amplitude fell to undetectable levels (Figure 6D). However, retinal histological analysis of these mice by light and electron microscopy revealed no retinal abnormalities (data not shown).

The visual phenotype is suppressed by a human RBP transgene

To prove that the visual impairment of the $RBP^{-/-}$ mice was due to the absence of RBP, we generated a mouse

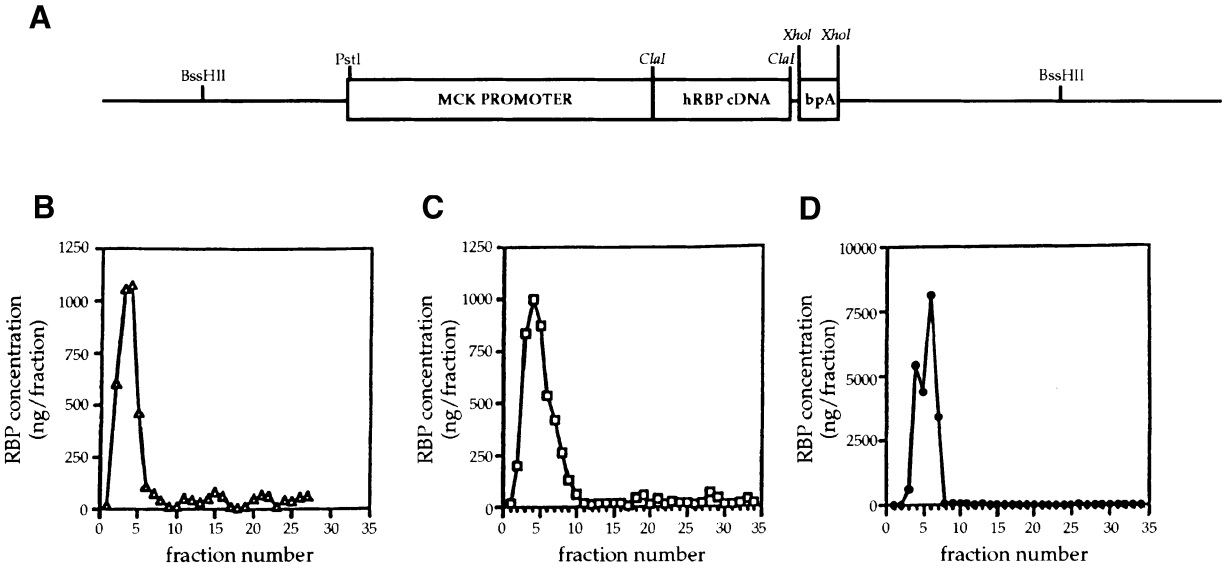

Fig. 7. Characterization of the MCK-hRBP mouse strain. (**A**) The MCK-hRBP construct used for microinjection is depicted. The construct was assembled from a human RBP cDNA (1 kb *Cla*I fragment), the promoter of the muscle creatine kinase gene (3.3 kb *Pst*I–*Cla*I fragment) and a bovine polyadenylation site (0.35 kb *Xho*I fragment) by conventional techniques. The positions of the *Bss*HII restriction sites defining the polylinker of the vector are also indicated. (B–D) Demonstration of binding between hRBP and TTR in the peripheral blood of the transgenic mice. Mouse serum (20 µl diluted to 1 ml in PBS) containing as size markers blue dextran (5 mg/ml) and cytochrome *c* (5 mg/ml) was size-fractionated on a 1×40 cm column of Bio-Gel P-100 flowing in PBS. Included fractions (~0.5 ml) were collected starting with the first fraction containing the blue dextran (fraction 1) and ending with the last fraction containing cytochrome *c* (fraction 35). The fractions were assayed by RIA for both hRBP and mRBP using specific antibodies (Blaner, 1990). The first RBP-containing-fraction (fraction 2) was the second to contain blue dextran and represents RBP bound to TTR. RBP not bound to TTR would elute in fractions 25–35. Note that the concentrations of hRBP in the peak fractions (maximum 5000 ng) were in the non-linear range of the RIA. (**B**) Elution profile observed for mRBP in wild-type serum: essentially all RBP is bound to TTR. (**C**) Elution profile for mRBP in MCK-hRBP transgenic serum: mRBP elutes in association with TTR. (**D**) Elution profile for hRBP in MCK-hRBP transgenic serum: hRBP elutes in association with TTR.

Table VI. Retinol, mRBP and hRBP levels in serum, liver and muscle from wild-type (wt) and MCK-hRBP transgenic (t) mice

Tissues	Retinol[a] (µg/dl)	Retinol[a] (µg/g)	mRBP[b] (mg/dl)	hRBP[c] (mg/dl)
Plasma				
t	57.0 ± 6.5		2.5 ± 0.2	7.0 ± 1.0
wt	18.1 ± 1.5		2.8 ± 0.6	–
Liver				
t		95.2 ± 30.6		
wt		77.7 ± 17.8		
Muscle				
t		1.29 ± 0.27		
wt		0.44 ± 0.31		

[a]Retinol levels are determined by reverse phase HPLC. [b]mRBP and [c]hRBP are determined by RIA. The values reported refer to four wild-type and four MCK hRBP male mice analyzed. Values are given as means ± SD.

strain that overexpressed human RBP cDNA under the control of the muscle-specific creatine kinase (MCK) promoter (Levak-Frank *et al*., 1995). Some of the characteristics of this transgenic strain are illustrated in Figure 7 and in Table VI; a fuller description will appear elsewhere (L.Quadro, W.S.Blaner, V.Colantuoni and M.E.Gottesman, in preparation). Human RBP is expressed in muscle but not in the liver or the eye cups for this transgenic mouse strain. The human RBP functions like the endogenous mouse RBP: it binds retinol, forms a complex with mouse TTR and transports vitamin A to target tissues (Figure 7). The transgenic animals were crossed with the $RBP^{-/-}$ mice to obtain a strain that overexpressed human RBP in the mouse RBP null background. Electroretinograms of such animals at 4 weeks of age were indistinguishable from those of wild-type mice (data not shown). Thus, human RBP entirely suppresses the visual impairment of the $RBP^{-/-}$ mice. This result confirms and extends the results with the $RBP^{+/-}$ mice which lack a visual phenotype. We conclude that the visual defect in the $RBP^{-/-}$ is indeed the result of RBP insufficency (and not, for example, due to some activity of the mutant protein).

Discussion

To understand the physiological role of RBP, we generated RBP knockout mice and followed these animals for 8 months. The mutant mice totally lack functional RBP but are viable and fertile. However, they show reduced levels of plasma retinol (12.5% of wild-type) and two other major defects: abnormal vision through the first several months of life and an inability to mobilize retinol from hepatic stores.

The viability and fertility of the $RBP^{-/-}$ animals was unexpected, since RBP is the sole specific carrier for retinol in the circulation of adult animals and in the developing embryo (Soprano and Blaner, 1994; Bavik *et al*., 1996; Johansson *et al*., 1997; Sapin *et al*., 1997; Barron *et al*., 1998). Evidently, there is plasticity in retinoid transport pathways. In fact, circulating retinoic acid levels (data not shown) and the uptake of chylomicron retinyl ester are normal in the knockout mice.

Normal vision and photoreceptor function require retinol and its specific eye metabolite, 11-*cis*-retinal. Vision is a critical physiological function in higher vertebrates, essential for survival and fitness in the wild. The impor-

tance of RBP in maintaining visual responsiveness is consistent with the high degree of homology of the RBP gene and the conservation of RBP protein and gene structure among different species. RBP knockout animals are born with impaired retinal function, but when fed a standard chow diet, which provides a sufficient and steady source of retinol, the animals acquire normal vision by 5 months of age. The $RBP^{-/-}$ mice are, therefore, able to use an alternative pathway(s) to acquire eye retinol. The alternative pathway(s) functions poorly *in utero* and early in life, since 21-day-old mice display low eye retinol levels (Figure 5A). However, the retinol content in the eye cups of the $RBP^{-/-}$ mice rises at the same rate as in $RBP^{+/+}$ animals after weaning (21 days; Figure 5A). Thus, the alternative pathway(s), which we believe derives retinol exclusively from recently ingested vitamin A, is adequate to maintain normal visual function in adult animals under laboratory conditions. However, eye retinol stores (retinyl ester) remain low in adult $RBP^{-/-}$ mice kept on a vitamin A-sufficient diet. This further supports the notion that the vitamin A status of these animals is extremely tenuous, particularly with respect to visual function.

TTR-deficient mice also have low circulating serum RBP and retinol levels (5 and 6% of wild-type, respectively) (Episkopou *et al*., 1993; Wei *et al*., 1995). However, dark-adapted ERGs from TTR-deficient mice, ranging in age between 3 weeks and 8 months post-partum, were normal (data not shown). Therefore, the absence of the retinol–RBP complex rather than low serum retinol levels *per se* must be responsible for the impaired retinal function observed in young $RBP^{-/-}$ animals. This raises the question of why young RBP knockout mice have insufficient eye retinol but normal retinol levels in other tissues. Several reports suggest that the RPE expresses a receptor for RBP (Bavik *et al*., 1993; Nicoletti *et al*., 1995; Tsilou *et al*., 1997) which presumably plays a role in the uptake of retinol. Our data clearly demonstrate an RBP-independent mechanism(s) for accumulating eye retinol. However, they do not resolve the question of whether RBP acts through a specific receptor to deliver retinol to the eye.

A knockout of the mouse RPE65 gene has been reported recently (Redmond *et al*., 1998). The mutant mice have a visual defect. Although once suggested to be the RBP receptor, the phenotype of the RPE65-deficient mouse argues against this notion. The biochemical phenotype of the RPE65-deficient mice is distinctly different from that which we have observed for RBP-deficient mice. The visual defect in the RPE65 mutants is, therefore, related to some function of RPE65 in vitamin A metabolism unrelated to a proposed action in facilitating RBP binding to or uptake by cells.

In addition to an insertion within *rbp*, our model mice carry an RBP rearrangement that yields a transcript that hybridizes with an RBP probe as well as a 28 kDa mutant protein. Although this protein reacts by Western immunoblot with one of two anti-RBP antibodies, it binds neither retinol nor TTR in the circulation of $RBP^{-/-}$ mice (see Figure 3). Moreover, within the circulation of $RBP^{-/-}$ mice, the 28 kDa protein is present as a high molecular weight aggregate and not as a monomer or bound to TTR. The existence of the 28 kDa mutant protein as a protein aggregate could account for the failure of the sheep anti-RBP antiserum used for RIA analysis to detect the protein under mild non-denaturing conditions whereas the rabbit anti-RBP antiserum used for Western blot analysis was able to detect the 28 kDa protein following denaturation and SDS–PAGE. Furthermore, N-terminal sequencing and very sensitive (with a low detection limit of <500 fmol per peptide fragment) MALDI-MS analysis of peptide fragments generated upon trypsin digestion of the 28 kDa protein revealed no substantial sequence resemblance between the 28 kDa protein and RBP. ERG analyses of $RBP^{+/+}$ and $RBP^{+/-}$ mice were indistinguishable, indicating that the rearrangement does not induce a gain-of-function mutation. Finally, the impaired retinal function, as assessed by ERG analysis of 4-week-old $RBP^{-/-}$ animals, was suppressed by a human RBP transgene expressed uniquely in skeletal muscle. Consequently, the phenotype of RBP knockout mice is due to the absence of functional RBP.

A similar phenotype recently has been observed in two sisters who lack serum RBP and display low serum retinol levels. The sisters have impaired vision as manifested by night blindness and altered rod function (Seeliger *et al*., 1999). Genetic analysis of the siblings indicates two compound heterozygous mutations in exons III and IV of the RBP gene, transmitted as a recessive trait (Biesalski *et al*., 1999). The visual phenotype reported and the impaired release of retinol from the liver stores, revealed by biochemical characterization of these two patients, are similar to what we describe here for the $RBP^{-/-}$ mice. Thus, our mouse strain could be a model for studying this genetic disorder and, eventually, for gene therapy.

The impaired retinal function is not associated with a developmental or structural abnormality in the retina. Indeed, the histology of retina from $RBP^{-/-}$ and $RBP^{+/+}$ mice at 4 weeks of age, as judged by light microscopy, was indistinguishable (data not shown). The absence of developmental defects in $RBP^{-/-}$ animals indicates that the fetus has sufficient levels of tissue retinoic acid. In fact, retinoic acid and retinol levels in whole newborn (1-day-old) RBP knockout and wild-type mice were identical (data not shown). That the retinoic acid levels are normal is not surprising, since, except for the eye, both fetal and adult $RBP^{-/-}$ animals maintain normal tissue retinol levels in the face of low plasma retinol concentrations.

We find of great interest the fact that by 5 months of age $RBP^{-/-}$ mice accumulate a significantly higher concentration of hepatic retinol than wild-type mice. Furthermore, that the hepatic levels of total retinol of these animals do not fall after a short-term exposure to a vitamin A-deficient diet indicates that $RBP^{-/-}$ mice cannot mobilize hepatic retinoid stores. This suggests that in times of inadequate vitamin A intake, RBP ensures that retinol is available for maintaining normal cellular function. This, we propose, is the major physiological role of RBP.

Materials and methods

Construction of targeting vector

A 0.5 kb RBP mouse cDNA *Eco*RI fragment lacking exon VI (obtained through the IMAGE Consortium, Mobile, AL) was used to isolate a 14 kb genomic DNA from a mouse λ FixII 129/Sv library. The targeting

vector was constructed by cloning a 6.5 kb *Eco*RI genomic fragment, extending from 1.5 kb upstream of the start site through the fourth intron, in a Bluescript IISK (–) plasmid in which the *Sma*I site of the polylinker region was eliminated by *Bam*HI–*Pst*I digestion. This recombinant plasmid was then digested with *Sma*I, to eliminate 591 bp of the *RBP* gene, and a 1.1 kb blunt-ended *Xho*I–*Hin*dIII fragment from the *PMC1neo poly(A)* gene (Episkopou *et al*., 1993) was inserted in the opposite orientation. In the 5′ position, a 1.85 kb *Xho*I–*Hin*d III blunt-ended fragment of the *PMC1tk* gene (Episkopou *et al*., 1993) was inserted, in the opposite orientation, into a unique *Not*I restriction site, also made blunt-ended. DNA was linearized with *Sac*II before use for electroporation in 129/Sv ES cells.

Generation of RBP$^{-/-}$ mice

ES cells were manipulated essentially as described previously (Belluscio *et al*., 1998). 129/Sv ES cells were electroporated with the construct and then placed under positive/negative selection with G418 and gancyclovir (Thomas and Capecchi, 1987). ES cell colonies surviving after 9 days were picked and their genomic DNA was digested with *Bam*HI, *Hin*dIII and *Eco*RI and hybridized with four different probes (see Results and Figure 1). Southern blot analysis was performed using 15 μg of digested genomic DNA, electrophoresed on a 0.8% agarose gel, treated with 0.25 M HCl for 15 min and blotted to Hybond N^+ (Amersham) by capillary transfer in NaOH 0.4 M for 3 h. Hybridizations were performed at 65°C for 3 h in Rapid-hyb Buffer (Amersham) and blots were washed three times at 65°C in 0.1× SSC, 0.1% SDS before autoradiography. ES cells from the resistant clone were expanded and used to generate chimeras by microinjection into C57BL/6J blastocysts (Papaioannou and Johnnson, 1993). Thirteen chimeric males were bred with C57BL/6J females. All showed germline transmission. Progeny were genotyped by Southern blot, heterozygous sibilings were interbred and the resulting F_2 and F_3 generations analyzed by Southern blotting. All the mice were in a mixed background (129×C57BL/6J).

RNA and protein analysis

RNA preparation and Northern blot analysis were performed as described (Sambrook *et al*., 1989); the mouse RBP cDNA described above was used as probe. Rabbit polyclonal anti-rat RBP antiserum (Muto *et al*., 1972) and rabbit polyclonal anti-rat TTR antiserum (Navab *et al*., 1977) were used for Western blot analysis performed according to standard procedures (Sambrook *et al*., 1989). Sheep polyclonal anti-rat RBP antiserum (Navab *et al*., 1977; Brouwer *et al*., 1988) was used for RIA performed as described (Blaner, 1990).

[^{3}H]Retinol binding assay in vivo

Six 3-month-old male RBP$^{+/+}$ and RBP$^{-/-}$ mice were used to assess the ability of the 28 kDa mutant protein to bind and transport retinol in the circulation. Each was given by gavage a dose consisting of 1 μCi of [^{3}H]retinol (55 Ci/mmol; New England Nuclear Life Sciences Products, Boston, MA) in 0.1 ml of peanut oil. Ten hours after administration of this dose, a time that is sufficient for all chylomicron retinyl ester to be cleared from the circulation of the mice (Weng *et al*., 1999), the mice were sacrified and pools of RBP$^{+/+}$ and RBP$^{-/-}$ serum containing [^{3}H]retinol were obtained. The serum pools (0.5 ml of each) were fractionated by gel exclusion chromatography, using a 1×50 cm column of Sephacryl S-200 (Pharmacia Amersham, Piscataway, NJ). The column was eluted with 10 mM sodium phosphate pH 7.2, containing 150 mM NaCl, and fractions consisting of 1.05 ml were collected. The Sephacryl S-200 column had been calibrated previously with blue dextran, bovine serum albumin (BSA) and cytochrome *c* to establish the void volume of the column and the included volumes for globular proteins with molecular masses of ~68 and 13 kDa. After chromatography, aliquots of each fraction were taken for analysis of ^{3}H c.p.m. by liquid scintillation counting and for RBP or the 28 kDa protein by immunoblot analysis as described above. After identification of fractions that contained ^{3}H c.p.m., all fractions from under a peak of ^{3}H c.p.m. were pooled for retinol analysis by HPLC, employing the procedures described below.

Purification and structural analysis of the 28 kDa protein by MALDI-MS and N-terminal sequence

To purify the 28 kDa protein for structural analysis, 1.2 ml of a serum pool obtained from six RBP$^{-/-}$ mice was mixed with 0.1 ml of protein A–Sepharose beads previously loaded with rabbit anti-rat-RBP IgG (4 mg IgG/1.2 ml beads). The mixing ratio of mouse serum and protein A–Sepharose used for immunoprecipitation was optimized previously through titration of the IgG–protein A–Sepharose with RBP$^{+/+}$ mouse serum. With these ratios of serum, IgG and protein A–Sepharose, we could immunoprecipitate a maximum amount of RBP from RBP$^{+/+}$ mouse serum. Immunocomplexes were obtained by incubation at 4°C overnight with gentle rotation. After incubation, the suspension was centrifuged in an Eppendorf centrifuge at 13 000 r.p.m. for 1 min, yielding a pellet and a supernatant. After removal of the supernatant, the pellet was washed three times with 1× phosphate-buffered saline (PBS) and, following the final wash, 2× SDS–PAGE treatment buffer equal in volume to the estimated pellet volume was added to the Eppendorf tube. After treatment of the pellet at 100°C for 5 min, the Eppendorf tube was centrifuged at 13 000 r.p.m. for 1 min and the supernatant was loaded onto a 12% SDS–polyacrylamide gel and electrophoresed at 40 mA for 6 h. A portion of the gel was then stained with Coomassie Blue to visualize the 28 kDa protein. The Coomassie-stained gel showed that the 28 kDa protein was the major protein band and that there were no other significant protein bands in the vicinity of the 28 kDa protein band. The portion of the unstained SDS–polyacrylamide gel corresponding to the 28 kDa band was excised carefully from the gel with a razor blade.

The 28 kDa protein was prepared for digestion by cutting the gel slice into small pieces and submerging them in 0.1 ml of 0.01 M dithiothreitol (DTT) in 0.1 M Tris–HCl pH 8.5 and shaking gently for 1 h at 55°C. The liquid was then removed from the tube and replaced with 0.1 ml of 0.015 M *N*-isopropyliodoacetamide/0.1 M Tris–HCl pH 8.5. After reaction for 30 min in the dark, the supernatant containing the alkylating reagent was removed and discarded. The gel pieces were washed with 0.5 ml of 0.05 M Tris–HCl pH 8.5/50% acetonitrile for 20 min with shaking. The supernatant was discarded and the wash step was repeated twice. Washed gel pieces were then dried completely in a Speed-Vac. After drying, 50 μl of digestion buffer (0.02 M Tris–HCl pH 8.5) containing 0.1 μg of trypsin (Boehringer Mannheim, sequencing grade) was added to the tube containing the dried gel and the tube was incubated for 20 h at 32°C. After digestion was complete, peptides were extracted by adding 100 μl of 50% acetonitrile/0.1% trifluoracetic acid (TFA), shaking for 30 min, and removing the supernatant to a clean tube. This extraction step was repeated once and 10% of the combined supernatants was dried on a Speed-Vac prior to analysis by MALDI-MS (Henzel *et al*., 1993). Matrix solution for MALDI analysis was prepared by making a 10 mg/ml solution of 4-hydroxy-α-cyanocinnamic acid in 50% acetonitrile/0.1% TFA and adding an internal standard (angiotensin) to the matrix. The dried digest was dissolved in 4 μl of matrix/standard solution and 0.8 μl was spotted on the sample plate. MALDI-MS analysis was performed on the digest using a PerSeptive Voyager DE-RP mass spectrometer in the linear mode.

The 28 kDa mutant protein, purified as described above, was loaded onto a 12% SDS–polyacrylamide gel, electrophoresed at 40 mA for 6 h and transferred onto a Problot membrane (ABI). After staining of the membrane with Coomassie Blue, according to the ABI protocol, the portion of the membrane containing the 28 kDa protein was excised, and the protein was eluted and subjected to automated N-terminal sequencing, as described (Ferrara *et al*., 1993).

Reverse and normal phase HPLC

Retinol and retinyl ester concentrations in plasma and tissues were measured by reverse phase HPLC as described (Blaner *et al*., 1987; Wei *et al*., 1995). 11-*cis*-retinal was measured in eye cups homogenates by normal phase HPLC (Mertz *et al*., 1997).

Electroretinograms

Dark-adapted ERGs were performed as previously described (Tsang *et al*., 1996). Dark-adapted ERG responses were obtained from anesthetized mice after their pupils were dilated with 1% phenylepinephrine HCl. A 30 gauge needle was placed subcutaneously on the forehead to serve as a reference electrode and a ground electrode was placed subcutaneously on the trunk. A saline-moistened cotton wick recording electrode was positioned to contact the cornea. Stimulating light flashes were obtained from a stroboscope (Grass Instruments Inc.). Neutral density filters were placed in front of the aperture to vary the intensity of the flashes. Responses were detected using an oscilloscope and an evoked response-detecting computer in parallel (Nicolet Instruments CA-100). All mice were dark-adapted overnight before ERGs were performed. Stimulation was begun with 4.8 log units of neutral density filtering and the responses were averaged to one flash every second. At high flash intensity, each flash was repeated every 20 s, an interval which, in preliminary experiments, was found to be sufficiently long to exclude interference of one flash on a later one. The duration of one flash was nominally 10 ms.

Diet

Purified retinol-deficient diet (W.F. Fisher & Son, Inc., Diet # 5822C-5I) contained <0.22 IU of retinol/g of diet; purified retinol-sufficient diet (W.F. Fisher & Son, Inc. Diet # 5755C-10I) contained 22 IU of retinol/g of diet. All other nutrients were present in the two purified diets at the same concentrations.

Acknowledgements

We thank A.Nemes for her excellent guidance and advice with ES cell technology, and X.Wu and W.Winston for their technical assistance. This work was funded by NIH grant R01DK50702.

References

Barron,M., McAllister,D., Smith,S.M. and Lough,J. (1998) Expression of retinol binding protein and transthyretin during early embryogenesis. *Dev. Dynam.*, **212**, 413–422.

Båvik,C.O., Levy,F., Hellman,U., Wernstedt,C. and Eriksson,U. (1993) The retinal pigment epithelial membrane receptor for plasma retinol-binding protein. Isolation and cDNA cloning of the 63-kDa protein. *J. Biol. Chem.*, **268**, 20540–20546.

Båvik,C., Ward,S.J. and Chambon,P. (1996) Developmental abnormalities in cultured mouse embryos deprived of retinoic acid by inhibition of yolk-sac retinol binding protein synthesis. *Proc. Natl Acad. Sci. USA*, **93**, 3110–3114.

Baylor,D. (1996) How photons start vision. *Proc. Natl Acad. Sci. USA*, **93**, 560–565.

Belluscio,L., Gold,G.G., Nemes,A. and Axel,R. (1998) Mice deficient in G_{olf} are anosmic. *Neuron*, **20**, 69–81.

Biesalski,H.K. *et al.* (1999) Biochemical but not clinical vitamin A deficiency results from mutations in the gene for retinol binding protein. *Am. J. Clin. Nutr.*, **69**, 931–936.

Blaner,W.S. (1990) Radioimmunoassays for retinol-binding protein, cellular retinol-binding protein, and cellular retinoic acid-binding protein. *Methods Enzymol.*, **189**, 270–281.

Blaner,W.S. and Olson,J.A. (1994) Retinol and retinoic acid metabolism. In Sporn,M.B., Roberts,A.B. and Goodman,D.S. (eds), *The Retinoids, Biology, Chemistry and Medicine.* Raven Press, New York, NY, pp. 229–256.

Blaner,W.S., Das,S.R., Gouras,P., Flood,M.T. (1987) Hydrolysis of 11-*cis* and all-*trans*-retinyl palmitate by homogenates of human retinal epithelial cells. *J. Biol. Chem.*, **262**, 53–58.

Brouwer,A., Blaner,W.S., Kukler,A. and van den Berg,K.J. (1988) Study on the mechanism of interference of 3,4,3′,4′,-tetrachlorobiphhenyl with the plasma retinol-binding proteins in rodents. *Chem.-Biol. Interact.*, **68**, 203–217.

Chen,J.D. and Evans,R.M. (1995) A transcriptional co-repressor that interacts with nuclear hormone receptors. *Nature*, **377**, 454–457.

Clagett-Dame,M. and Plum,L.A. (1997) Retinoid-regulated gene expression in neural development. *Crit. Rev. Euk. Gene Expr.*, **7**, 299–342.

Episkopou,V., Maeda,S., Nishiguchi,S., Shimada,K., Gaitanaris,G.A., Gottesman,M.E. and Robertson,E.J. (1993) Disruption of the transthyretin gene results in mice with depressed levels of plasma retinol and thyroid hormone. *Proc. Natl Acad. Sci. USA*, **90**, 2375–2379.

Ferrara,P., Rosenfeld,J., Guillemot,J.C. and Capdeville,J. (1993) Internal peptide sequence of proteins digested in gel after one- or two-dimensional gel electrophoresis. In Angeletti,R.H. (ed.), *Techniques in Protein Chemistry IV.* Academic Press, San Diego, CA, pp. 379–387.

Goodman,D.S. (1984) Vitamin A and retinoids in health and disease. *N. Engl. J. Med.*, **310**, 1023–1031.

Gudas,L.J., Sporn,M.B. and Roberts,A.B. (1994) Cellular biology and biochemistry of the retinoids. In Sporn,M.B., Roberts,A.B. and Goodman,D.S. (eds), *The Retinoids, Biology, Chemistry and Medicine.* Raven Press, New York, pp. 443–520.

Gregory-Evans,K. and Bhattacharya,S.S. **(**1998) Genetic blindness: current concepts in the pathogenesis of human outer retinal dystrophies. *Trends Genet.*, **14**, 103–108.

Helms,R.A., Dickerson,R.N., Ebbert,M.L., Christensen,M.L. and Herrod,H.G. (1986) Retinol-binding protein and prealbumin: useful measures of protein repletion in critically ill, malnourished infants. *J. Pediatr. Gastr. Nutr.*, **5**, 586–592.

Henzel,W.J., Billeci,T.M., Stults,J.T., Wong,S.C., Grimley,C. and Watanabe,C. (1993) Identifying proteins from two-dimensional gels by molecular mass searching of peptide fragments in protein sequence database. *Proc. Natl. Acad. Sci. USA*, **90**,5011–5015.

Holm,J., Hemmingsen,L. and Nielson,N.V. (1988) Relationship between the urinary excretion of albumin and retinol-binding protein in insulin-dependent diabetics. *Clin. Chim. Acta*, **177**, 101–105.

Johansson,S., Gustafson,A.L., Donovan,M., Romert,A., Eriksson,U. and Dencker,L. (1997) Retiniod binding proteins in mouse yolk sac and chorio-allantoic placentas. *Anat. Embryol. (Berl.)*, **195**, 483–490.

Kelsey,C.A. (1997) Detection of vision information. In Hendee,W.R. and Wells,P.N.T. (eds), *The Perception of Visual Information*. Springer-Verlag, New York, NY, pp. 33–56.

Kurokawa,R., Soderstrom,M., Horlein,A., Halachmi,S., Brown,M., Rosenfeld,M.G. and Glass,C.K. (1995) Polarity-specific activities of retinoic acid receptors determined by a co-repressor. *Nature*, **377**, 451–454.

Leblanc,B.P. and Stunnenberg,H.G. (1995) 9-*cis* retinoic acid signaling: changing partners causes some excitement. *Genes Dev.*, **9**, 1811–1816.

Levak-Frank,S. *et al.* (1995) Muscle-specific overexpression of lipoprotein lipase causes a severe myopathy characterized by proliferation of mitochondria and peroxisomes in transgenic mice. *J. Clin. Invest.*, **96**, 976–986.

Mangelsdorf,D.J. *et al.* (1995) The nuclear receptor superfamily: the second decade. *Cell*, **83**, 835–839.

Marks,F., Piantedosi,R., Blaner,W.S., Dancis,J., Lavitz,M. and Goodman,D.S. (1991) Studies of the temporal and anatomic patterns of expression of retinol-binding protein (RBP), cellular retinol-binding protein (CRBP), and transthyretin (TTR) in human placenta. *FASEB J.*, **5**, A717.

Matsuo,T., Matsuo,N., Shiraga,F. and Koide,N. (1987) Familial retinol-binding-protein deficiency. *Lancet* **2**, 402–403.

Mertz,J.R., Shang,E., Piantedosi,R., Wei,S., Wolgemuth,D.J. and Blaner,W.S. (1997) Identification and characterization of a stereo-specific human enzyme that catalyzes 9-*cis*-retinol oxidation. *J. Biol. Chem.*, **272**, 11744–11749.

Monaco,HL., Rizzi,M. and Coda,A. (1995) Structure of a complex of two plasma proteins: transthyretin and retinol-binding protein. *Science*, **268**, 1039–1041.

Morriss-Kay,G.M. and Sokolova,N. (1996) Embryonic development and pattern formation. *FASEB J.*, **10**, 961–968.

Muto,Y., Smith,J.E., Milch,P.O. and Goodman,D.S. (1972) Regulation of retinol-binding protein metabolism by vitamin A status in the rat. *J. Biol. Chem.*, **247**, 2542–2550.

Napoli,J.L. (1996) Biochemical pathways of retinoid transport, metabolism, and signal transduction. *Clin. Immunol. Immunopathol.*, **80**, S52–S62.

Navab,M., Mallia,A.K., Kanda,Y. and Goodman,D.S. (1977) Rat plasma prealbumin. Isolation and partial characterization. *J. Biol. Chem.*, **252**, 5100–5106.

Newcomer,M.E. (1995) Retinoid-binding proteins: structural determinants important for function. *FASEB J.* **9**, 229–39.

Nicoletti,A., Wong,D.J., Kawase,K., Gibson,L.H., Yang-Feng,T.L., Richards,J.E. and Thomposon,D.A. (1995) Molecular characterization of the human gene encoding an abundant 61 kDa protein specific to the retinal pigment epithelium. *Hum. Mol. Genet.*, **14**, 641–649.

Papaioannou,V.E. and Johnnson,R. (1993) Production of chimeras and genetically defined offspring from targeted ES cells. In Joyner,A.L. (ed.), *Gene Targeting.* Oxford University Press, New York, NY, pp. 107–146.

Pfahl,M. and Chytil,F. (1996) Regulation of metabolism by retinoic acid and its nuclear receptors. *Annu. Rev. Nutr.*, **16**, 257–283.

Redmond,T.M. *et al.* (1998) Rpe65 is necessary for production of 11-*cis*-vitamin A in the retinal visual cycle. *Nature Genet.*, **20**, 344–351.

Sambrook,J., Fritsch,E.F. and Maniatis,T. (1989) *Molecular Cloning: A Laboratory Manual*. 2nd edn. Cold Spring Harbor Laboratory Press, Cold Spring Harbor, NY.

Sapin,V., Ward,S.J., Bronner,S., Chambon,P. and Dollé,P. (1997) Differential expression of transcripts encoding retinoid binding proteins and retinoic acid receptors during placentation of the mouse. *Dev. Dynam.*, **208**, 199–210.

Seeliger,M.W., Biesalski, H.K., Wissinger,B., Gollnick,H., Gielen,S., Frank,J., Beck,S. and Zrenner,E. (1999) Phenotype in retinol deficiency due to a hereditary defect in retinol binding protein syntesis. *Invest. Ophthalmol. Visual Sci.*, **40**, 3–11.

Soprano,D.R. and Blaner,W.S. (1994) Plasma retinol-binding protein. In Sporn,M.B., Roberts,A.B. and Goodman,D.S. (eds), *The Retinoids, Biology, Chemistry and Medicine*. Raven Press, New York, NY, pp. 257–282.

Thomas, K.R. and Capecchi, M.R. (1987) Site-directed mutagenesis by gene targeting in mouse embryo-derived stem cells. *Cell*, **51**, 503–512.

Tsang,S.H., Gouras,P., Yamashita,C.K., Kjeldbye,H., Fisher,J., Farber,D.B. and Goff,S. (1996) Retinal degeneration in mice lacking the γ subunit of the rod cGMP phosphodiesterase. *Science*, **272**, 1026–1029.

Tsilou,E., Hamel,C.P., Yu,S. and Redmond,T.M. (1997) RPE65, the major retinal pigment epithelium microsomal membrane protein, associates with phospholipid liposomes. *Arch. Biochem. Biophys.*, **346**, 21–27.

Vogel,S., Gamble,M.V. and Blaner,W.S. (1999) Biosynthesis, absorption, metabolism and transport of retinoids. In Nau,H. and Blaner,W.S. (eds), *Handbook of Experimental Pharmacology, Retinoids*, Springer-Verlag, Heidelberg, Germany, pp. 31–95.

Wald,G. (1968) The molecular basis of visual excitation. *Nature*, **219**, 800–807.

Wei,S., Episkopou,V., Piantedosi,R., Maeda,S., Shimada,K., Gottesman,M.E. and Blaner,W.S. (1995) Studies on the metabolism of retinol and retinol-binding protein in transthyretin-deficient mice produced by homologous recombination. *J. Biol. Chem.*, **270**, 866–870.

Weng,W., Li,L., van Bennekum,A.M., Potter,S.H., Harrison,E.H., Blaner,W.S., Breslow,J.L. and Fisher,E.A. (1999) Carboxyl ester lipase knockout mice have partially decreased intestinal absorption of dietary cholesteryl ester and normal retinyl ester absorption. *Biochemistry*, **38**, 4143–4149.

Winkler,M.F., Gerrior,S.A., Pomp,A. and Albina,J.E. (1989) Use of retinol-binding protein and prealbumin as indicators of the response to nutrition therapy. *J. Am. Diet. Assoc.*, **89**, 684–687.

Received March 29, 1999; revised and accepted July 5, 1999